Renewable Energy 219 (2023) 119466

Contents lists available at ScienceDirect

Renewable Energy

journal homepage: www.elsevier.com/locate/renene

Digital twin-based optimization and demo-scale validation of absorption columns using sodium hydroxide/water mixtures for the purification of biogas streams subject to impurity fluctuations

Jacopo Pallavicini [a], Matteo Fedeli [a,b], Giacomo Domenico Scolieri [a], Francesca Tagliaferri [a], Jacopo Parolin [c], Selena Sironi [a], Flavio Manenti [a,*]

[a] Politecnico di Milano, Dipartimento di Chimica, Materiali ed Ingegneria Chimica "Giulio Natta", Piazza Leonardo da Vinci 32, 20133, Milano, Italy
[b] Laboratoire de Génie Chimique, Université de Toulouse, CNRS/INP/UPS, Toulouse, France
[c] Tecnoimpianti Water Treatment srl, Via Salvo D'Acquisto, 16/B, 20060, Pozzuolo Martesana (MI), Italy

ARTICLE INFO

Keywords:
Digital twin
Process optimization
H_2S removal
Biogas purification
Demo-scale campaign

ABSTRACT

This paper aims to validate a demo scale plant scrubber technology through experimental campaign and development of a digital twin. Thus, it is useful to evaluate the H_2S absorption process in a biogas production plant for analysis and optimization purposes. The absorber unit removes H_2S through the chemical absorption via sodium hydroxide (NaOH) as wet agent (30% w/w). The column treats 300 Nm^3/h of biogas, whose inlet H_2S concentration ranges from 1000 to 3000 ppm. Field measurements are conducted to investigate the H_2S removal efficiency. An experimental dataset is collected, processed and used as input on Aspen PLUS suite to develop the digital twin.

This model is helpful to generate a large dataset and simulate operating conditions different from the demo-scale plant. The process simulation is then exploited to perform a sensitivity analysis to figure out main variables influencing the H_2S removal efficiency. Operating conditions such as H_2S concentration, soda concentration and flowrate, temperature, and freshwater flowrate are perturbed in the sensitivity analysis. NaOH flowrate and its concentration are the variables with the biggest impact on the process. In detail, the highest efficiency performance was obtained using 50% NaOH solution with a flowrate higher than 8 kg/h.

1. Introduction

Biogas is the gaseous product obtained through a biochemical process known as anaerobic digestion. In this process, organic matter is decomposed in absence of oxygen by various types of anaerobic microorganisms. The obtained product is a methane-rich gas that can be further used for cooking, heating, and electricity generation [1]. New frontiers suggest its utilization as feedstock for the synthesis of biofuels through the Heat, Power, and Chemicals process [2]. Anaerobic digestion feedstocks include agricultural and household waste, livestock manure, landfill residues, and wastewater sludge [3]. Biogas typically contains about 50–70% methane (CH4), 30–50% carbon dioxide (CO2), and other trace impurities [4]. Anaerobic digestion is also a very interesting process because methane is stocked and used as an energy source and it is not emitted as landfill gas [5]. Thus, it led to an important reduction in methane emissions considering its stronger contributions as a greenhouse gas. The released methane has over 20–times more global warming effects than CO2 for a 100-year time horizon [6]. In recent years, the research focusing on alternative sustainable energies has significantly favoured the increasing of number of biogas plants. Biogas is included in the directive 2009/28/EC which establishes a network for energy promotion from renewable non-fossil sources [7,8]. A recent investigation estimated that the total amount of medium and large-scale biogas plants operating in the world is around 132′000 [9]. As previously mentioned, biogas contains small amounts of different contaminants that must be carefully kept under control such as hydrogen sulphide, ammonia, oxygen, nitrogen, water, and siloxanes [10]. Hydrogen sulphide is always present in biogas streams since it is produced during the transformation of sulphur-containing proteins and sulphates in the fermentation chamber [11]. However, the concentration of H2S in biogas is strictly dependent by the feedstock type, as shown in Fig. 1 [12].

* Corresponding author.
E-mail address: flavio.manenti@polimi.it (F. Manenti).

https://doi.org/10.1016/j.renene.2023.119466
Received 6 April 2023; Received in revised form 9 September 2023; Accepted 13 October 2023
Available online 14 October 2023

H_2S, even in small amounts, is lethal for human health; for instance, above 50 ppm, this contaminant may irritate the respiratory tract. Furthermore, hydrogen sulphide has a very low smell threshold (on the order of ppb), which might cause olfactive annoyance to the community near a biogas farm [14]. The World Health Organization recommends not to exceed the level of 7 $\mu g/m^3$ of H_2S (about 0.005 ppm) for the mean ambient air concentration measured over 30 min to avoid local disturbance [15]. Hydrogen sulphide represents a huge problem also in process plant engineering. It becomes potentially dangerous for process equipment and the environment. Moreover, biogas H_2S content above 1000 ppm damages all metal parts by strong corrosion called Sulfide Stress Cracking (SSC). This phenomenon is defined as induced cracking under the combined effect of tensile stress and atomic hydrogen adsorption and absorption [16]. Iron and non-ferrous metals components can be both attacked causing failures in gas engines, valves, compressors, and pressure regulators [17]. An additional effect of the H_2S is its further combustion within an oxygen-rich system with the production of SO_2. This compound reacts with water, forming sulphuric acid that corrodes burners unit and gas lamps [18]. In addition, if the SO_2 produced during combustion is dispersed in the atmosphere, it increases environmental pollution by causing acid rain [11]. H_2S catalyst poisoning is considered another critical effect in the process operations where this compound is present. Nickel and iron catalysts activity is strongly affected by the presence of H_2S leading to lower overall process performances [19]. H_2S poisoning is also reported for many catalysts used in downstream processes [20]. Currently, industrial-scale plants apply several technologies to remove H_2S from a gas stream [21]. Hence, biogas H_2S purification is strictly required for electricity production, fuel production, or its injection in the natural gas grid [22]. Innovative purification methods involve the adsorption of hydrogen sulphide on NaX and Ag-exchanged NaX zeolites [23]. These technologies are still in the lab-scale validation despite the removal efficiency being very high. Schiavon et al. [24] in their work obtain a 99% H_2S removal efficiency using a regenerable Fe-EDTA solution. Cristiano et al. [25] performed an H_2S adsorption on nanostructured iron oxide at room temperature. The result of their work is very promising despite the technology is only tested in a bench scale.

Caustic scrubbing with sodium hydroxide is one of the most extensively applied processes for removing H_2S and other acid species from gases. The scrubbing process of acid gases such as CO_2 and H_2S is applied for several reasons such as improving the calorific value of biogas streams and avoiding corrosion in process lines and fittings [26]. The lowest price of sodium hydroxide among different H_2S scavenging chemicals has led caustic scrubbing to be an economic and viable option for biogas desulphurization. However, the presence of CO_2 in the raw gas is critical for caustic scrubbers. High biogas CO_2 content strongly affects caustic scrubbing because this compound reacts with caustic medium with the formation of by-products such as sodium carbonate solids [27]. Special designs have been developed to allow H_2S to be scrubbed preferentially while slipping most of the CO_2 in the gas. These technologies exploit the lower chemical adsorption rates of CO_2 than H_2S in caustic mixtures. Shorter scrubbing contact time favors higher selectivity toward H_2S adsorption [28].

This work proposes the model validation of a demo-scale plant for the H_2S removal technology from biogas. Lack of works in literature deal with the analysis of H_2S caustic scrubbing from biogas, especially regarding pilot plants.

Experimental campaigns are useful to measure and test the process efficiency in nominal conditions. A dataset of new experimental data is collected from the demo scale plant. To investigate the behavior of the plant in perturbed conditions, such as H_2S fluctuations, a digital twin is realized. Moreover, digital twin is able to reproduce a large deviations of H_2S concentration. The process is rigorously simulated in Aspen PLUS using as model input the experimental results.

One of the most promising technologies for smart manufacturing and Industry 4.0 is digital twin (DT). Both academia and industry acknowledge the importance of DTs. A digital twin (DT) is a physical product, a virtual product, and a connection between physical and virtual products that connects the physical and digital worlds. The DT environment allows for real-time decisions and quick analysis using accurate analytics. Organizations can use DT and clever algorithms to produce sophisticated products and facilities, as well as increase business models and value generation [29,30].

A process digital twin could be used to (i) quickly generated large data output (ii) simulate operating conditions seldomly not replicable in the real plant, and (iii) prevent any safety risk [31]. Furthermore, the digital twin allows a system test under different conditions and predicts the demo-scale flexibility. The biogas inlet H_2S concentrations were set as system disturbances. This parameter is subject to periodical fluctuations due to different biogas treating conditions, local H_2S peak formations, and different purification scales. A sensitivity analysis is performed to highlight the most impactful variables in the biogas H_2S caustic scrubbing. The final purpose of the work is to validate the scrubbing technology in the demo-scale plant and optimize it for the further upscaling.

2. Materials and Methods

2.1. Pilot plant description

The H_2S removal via absorption with NaOH is tested in a demo-scale biogas production plant with a capacity of 300 Nm^3/h, located in

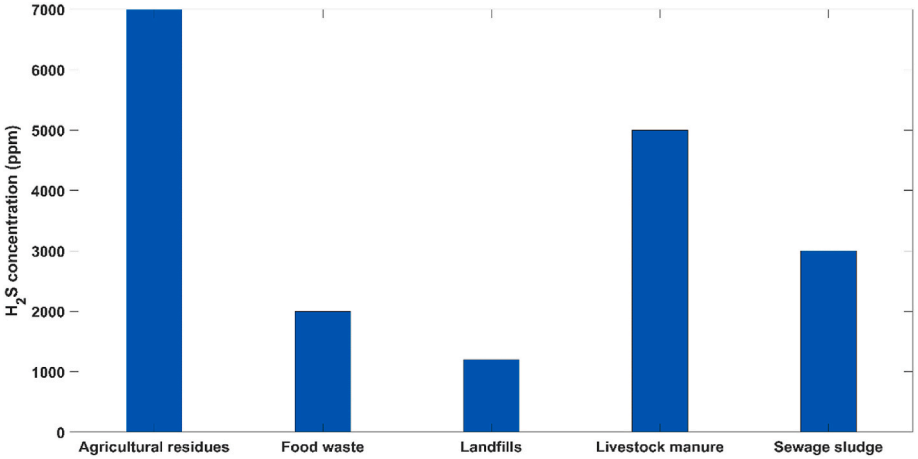

Fig. 1. Average H_2S concentration after biogas anaerobic digestion with different feedstock [13].

northern Italy. The plant includes a section for feedstock and digestate storage, a primary digester, a post-digester, an upgrading section, and a cogeneration section. The scrubbing unit is the focus of this work; the other components are not included in the research. Due to the high H_2S levels (1000–3000 ppm) in biogas, the plant is equipped with an upgrading section. The scrubbing unit is placed before the biogas injection in the cogeneration section, where unexpected impurities could generate failures. According to the manufacturer specifications, H_2S limits range from 1000 ppm (stationary engine) to 250 ppm (boiler), and then to 5 ppm (fuel cell) [32].

The range of H_2S levels is subject to fluctuations due to the digestor operating

Conditions. The main problem to figure out is the formation of solid crusts in the digestor. Indeed, when the feedstock (poultry manure added with pig and bovine manure) is pumped in the digester, solid crusts might form. This is an undesired phenomenon, since crusts may alter the process of biogas production possibly trapping biogas. The biogas acid gas is abruptly released when these crusts break. This phenomenon leads to fluctuations in inlet biogas H_2S fraction. The purpose of the experimental campaign is to validate the scrubbing technology with H_2S concentration uncertainty before transferring the unit to a bigger capacity plant. In the up-scale process, different operating conditions are expected. Thus, they could be (i) higher biogas flowrate, (ii) higher biogas H_2S inlet concentrations, (iii) different temperatures, and (iv) different digester operating conditions. An associated digital twin is useful to simulate all these conditions not replicable in the demo-scale plant. This model is helpful to simulate the response of the process in situation of crust breakage f and evaluate the scrubbing working efficiency. The former event results in large deviations from nominal conditions of H_2S concentration in biogas.

Fig. 2 shows the scrubbing column employed for H_2S removal.

The scrubbing technology is procured and designed by the company TecnoImpianti Water Treatment srl.

The column, with a height of 3.0 m and a diameter of 0.8 m, processes the outlet biogas stream from the digesters continuously. Fig. 3

Fig. 2. Absorption column of the plant.

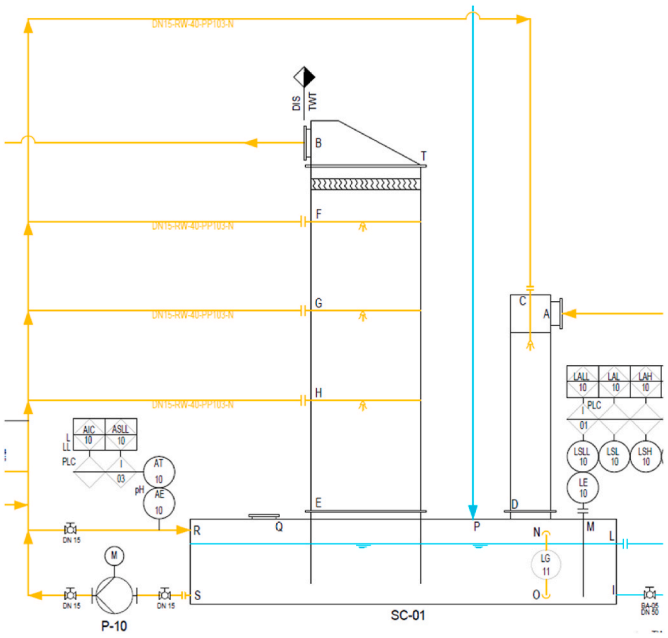

Fig. 3. P&ID of the absorption column.

depicts the P&ID of the absorber unit. The diagram includes a pre-washing column, a main column, and a bottom tank. The pre-washing column (Ø 0.2 m x H 1.2 m) is a single-nozzle configuration operated in co-current. The main column is equipped with three nozzles, which are operated in a counter-current to increase the removal efficiency. A grid at the bottom of the unit is used as packing support while a demister is placed on the top. Thus, it prevents liquid droplet entrainment by clean biogas. The scrubber unit is built in polyethylene following the ATEX norm to avoid potential explosive atmospheres. The washing solution sprayed by the nozzles is made of a mixture of freshwater and fresh sodium hydroxide (NaOH). Freshwater is taken from the national grid at a temperature of 10–15 °C, and it is directly added to the bottom tank. An external flowmeter controls the flowrate. The fresh sodium hydroxide (30% or 50% w/w) is stored in tanks at atmospheric conditions The concentration is referring to the value of undiluted solution.

The NaOH flowrate that enters before the column nozzles is controlled by a dosing pump. The discharge of unreacted NaOH falls into the bottom tank. This stream is partially discharged by a fixed weir, while the remaining part (~6 m^3/h) is recycled back to the nozzles mixed with the freshwater. Additional activated carbon filters are present after the scrubber to prevent any H_2S inlets in the cogeneration section.

2.2. Experimental campaign

A campaign of field measurements is conducted to study the H_2S removal efficiency in the caustic scrubber. The inlet and outlet positions of the scrubbing unit are taken as sampling points to measure H_2S concentration. Removal efficiency (η) is used as a key performance indicator to assess the scrubber performances. This parameter is defined as:

$$\eta\,[\%] = \frac{C^{IN}_{H_2S} - C^{OUT}_{H_2S}}{C^{IN}_{H_2S}} \bullet 100 \quad (1)$$

where $C^{IN}_{H_2S}$ and $C^{OUT}_{H_2S}$ are the inlet/outlet H_2S concentration (ppm) of the processed biogas. Inlet and outlet samples are collected contemporaneo usly in two Nalophan™ (PET, Polyethylene terephthalate) bags with a capacity of 6 L, ending with a Teflon® tube and cap. Sampling is carried

out through a vacuum pump which allows gases to flow into the sampling bag. Then, H_2S concentration is measured with a manual analyser (MRU Optima 7 - Biogas) equipped with a dedicated electrochemical sensor.

Tests are carried out during a 5-day experimental campaign. The upstream sections are tested in different operating conditions. Freshwater flowrate, sodium hydroxide flowrate and concentrations are perturbed. In Table 1 the operating conditions of the different trial days are shown. Note that the NaOH concentration values [% w/w] in Table 1 refer to the undiluted solution, before dilution with freshwater. The associated removal efficiencies of these trials are reported in the Results and Discussions section.

2.3. Digital twin modelling

The experimental campaign data are filtered and used as input for the detailed process simulation. The outliers are manually removed in case of physical unfeasibility and inconsistency. Commercial package tool Aspen PLUS® is employed for digital twin modelling. Electrolyte NRTL model has been adopted, whereas the Redlich-Kwong equation has been employed for the vapor phase. These thermodynamic methods are suitable to represent the liquid phase non-idealities as suggested by Cherif et al. [33]. A rate-based calculation type is selected despite the equilibrium-stage theory being extensively employed in the past years by chemical companies. The selected approach is more suitable to handle solid formation and chemical reactions occurring. Component properties such as activity coefficients, heat capacity, viscosity and density have been directly evaluated by Aspen Plus tool. Henry's constants for CH_4 CO_2, O_2 and H_2S are retrieved from the National Institute of Standards and Technology (NIST) databases. The temperature dependence of Henry's constant used by Aspen Plus® is represented by Eq. (2). Coefficients a_{ij}, b_{ij}, c_{ij}, d_{ij}, e_{ij} and the upper and lower temperature limits for each system are reported in the *Appendix* (Table A 1). The reacting system involves equilibrium, dissociation and kinetic reactions that are also reported in the *Appendix*. The selected set of reactions counts for thirteen reactions. Additional side reactions are not considered to limit the model complexity.

Concerning the equilibrium reactions, Aspen Plus® uses the expression reported in Eq. (3) to estimate the equilibrium constants. Power-law equation (Eq. (4)) has been utilised to define the reaction rate of kinetically controlled reactions (R12 and R13) in *Appendix*.

$$\ln H_{ij} = a_{ij} + \frac{b_{ij}}{T} + c_{ij} \ln T + d_{ij} T + \frac{e_{ij}}{T} \tag{2}$$

$$\ln K_{eq} = A + \frac{B}{T} + C \ln T + D\,T + \frac{E\left(P - P_{ref}\right)}{P_{ref}} \tag{3}$$

$$r = k\,T^{n}\,e^{\left(\frac{-E}{RT}\right)} \prod_{i=1}^{N} C_i^{a_i} \tag{4}$$

Where H_{ij} is the Henry's law constant for solute i in solvent j, K_{eq} is the equilibrium constant, r is the rate of reaction, k is a pre-exponential factor, T is the temperature, n is a temperature exponent, E is the activation energy, R is the universal gas constant, C_i is the concentration of component i, and a_i is the stoichiometric coefficient of component i in the reaction. The kinetic parameters k and the activation energy E for the two kinetically controlled reactions are reported in Table 2 [34]. R12 and R13 represent the direct and indirect kinetic formation of HCO_3^- ions. Thus, it led to carbonate precipitation in the unit.

The final layout implemented in the Aspen Plus® simulator is reported in Fig. 4 and it is discussed in the section below.

A solution of NaOH (30% or 50% w/w) diluted with a stream of freshwater is pumped and equally split into four different streams (S1–S4). S1, S2, and S3 enter in the "ABSORB2" while S4 is fed in the "ABSORB1". "ABSORB1" represents the pre-washing column while "ABSORB2" is the model of the main column absorber. The demo-scale scrubber unit is modelled with two in-series absorbers. Columns are implemented with the RADFRAC model. The RADFRAC model, short for "Rigorous Distillation Column Simulation," is a modeling and simulation tool used in the field of chemical engineering, particularly in the design and analysis of distillation columns. It is a type of dynamic simulation model that is employed to simulate the behavior of distillation columns under various operating conditions [35]. The geometry properties and operating conditions of these units are represented in Table 3. The biogas stream enters the bottom of "ABSORB1", goes through a cleaning process and exits from the top. Afterwards, the gas stream is fed from the bottom of the primary scrubbing column (ABSORB2). The pre-washing column is fed only with one solvent stream (S4), while the main column has three inlet solvent streams (S1, S2, and S3) for the three nozzles. The ABSORB2 internal type is packed with a 2-inch metallic pall ring according to the real column structures. The two columns discharge the liquid solution from the bottom through the two streams BOTTOM1 and BOTTOM2. To check the internal column status, the hydraulic plots are analysed. The adsorber operating point corresponds to 483,7 N/m^3. Liquid and gas mass flowrates are 0.43 and 0.19 kg/s respectively. No weeping and flooding phenomena are reported in the adsorber model.

MIXER2 unit represents the bottom fresh tank of the adsorption column. The mixer unit collects columns disengagement and mixes them with freshwater make-up (WATER). Part of the mixer outlet is purged in the "SPLIT2" thanks to the splitter unit. The purge ratio is 8% to guarantee sufficient stream recycling. The recycle stream is mixed with fresh NaOH, pumped, and split into the four streams of the cycle loop. In the real plant, the upgraded biogas exits the main scrubber by passing through the demister and is sent to a chiller for water removal. The demister and the chiller in the simulation are represented by the condenser (COND) and the flash (FLASH). The biogas stream, before entering the cogeneration plant, goes in a blower represented on Aspen Plus® by the compressor (COMPRESS).

It is noteworthy that ABSORB1 is modelled as countercurrent scrubber despite the real pre-washing column has a parallel flow between caustic agent and biogas. However, the RADFRAC model for this unit is computed with one stage equibrium. The choice of the flows is useless for the mathematical results since both streams enter in the same stage.

3. Results and discussions

3.1. Base-case scenario and alternative scenarios

The results of the different experimental trials are shown below in Table 4. H_2S inlet and outlet concentration are monitored to compute the removal efficiency.

The findings of the experimental campaign show that the sodium

Table 1
Operating condition of the upstream section during different experimental trials.

Trial days	NaOH [w/w %]	NaOH flowrate [L/h]	H_2O flowrate [L/h]
1	30	8	80
2	30	10	160
3	50	6	100
4	50	6	160
5	50	8	160

Table 2
Pre-exponential factor and activation energy for reactions 12 and 13.

Reaction	k	E (cal/mol)
R12	4.32 E+13	13249
R13	2.83 E+17	29451

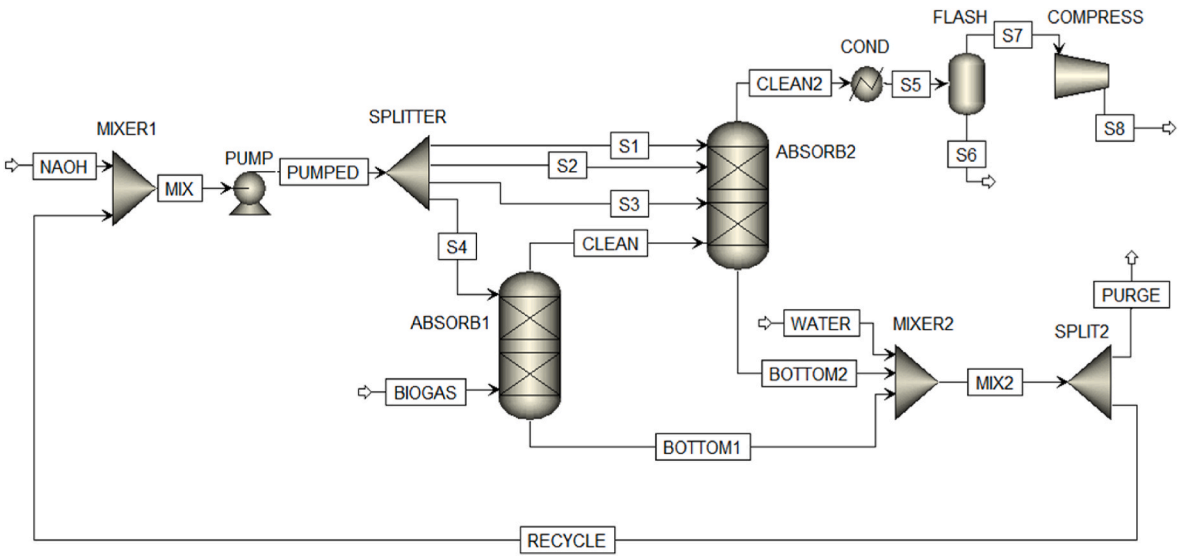

Fig. 4. Complete simulation layout.

Table 3
Main properties and operating conditions of the pre-washing column and main column.

Unit	Type	Section packed height/Diameter	Operating conditions
ABSORB1	Packed	0.8 m/0.3m	36.0 °C-1.1 bar
ABSORB2	Packed	2.2 m/0.3 m	34.8 °C- 1.1 bar

Table 4
Result of the experimental trials.

Trial days	H_2S inlet concentration [ppm]	H_2S outlet concentration [ppm]	η
1	1500	1200	20%
2	2500	1750	30%
3	1800	900	50%
4	2000	800	60%
5	2000	600	70%

hydroxide content, as well as its flow and freshwater flow, influenced the chemical absorption of H_2S. Low efficiency is achieved in the first two trials (i.e. 20%, 30%). This is most likely owing to the low concentration of sodium hydroxide (Table 1). Subsequent trials (#3, #4, #5), carried out with a higher solvent concentration, show a considerable increase in the removal efficiency up to 70%.

Moreover, by comparing trial #4 and trial #5, in which NaOH concentration and freshwater flow rate remain constant, lower outlet concentrations are achieved by increasing the sodium hydroxide flow rate. As a result, removal efficiency increases from 60 to 70%. Trial #3 and Trial #4 highlight the influence of water flowrate. In this case, by keeping constant NaOH flowrate and concentration, efficiency passes from 50% to 60%.

Based on collected experimental results, the highest efficiency (i.e. 70%) is achieved in trial #5 with the following operating conditions.

- NaOH concentration: 50%
- NaOH flowrate: 8 L/h
- Freshwater flow:160 L/h

Therefore, this test is adopted as a base-case scenario to model the digital twin. All the data collected during trial #5 are summarized in the tables below, i.e., process stream inlet composition and operating conditions. These data are used as input for the simulation. H_2S inlet concentration is characterized with the averaged value of the different field measurements. The output removal efficiency of the model is 71.2%, which is quite near the result measured during field experiments. Table 5 shows the main operating conditions and the compositions of the process simulation. The mass and energy balances of the wide plant are reported in the *Appendix* section. After this first test (base-case scenario), the accuracy of the model was also verified by conducting further simulations in the same operating conditions of the experimental campaign for field trials #1, #2, #3, and #4. To verify the digital twin reliability, experimental and process simulation H_2S removal efficiency data are compared. Relative error (%) is used as a key performance indicator of the model accuracy. The discrepancy between experimental data and digital twin is low with a maximum relative error of 5.77%. Table 6 highlights the removal efficiency for the digital twin and experimental campaign. The process simulation can be considered a digital twin of the process and can be exploited to collect and generate data. Thus, it will be used in the next section to perform the sensitivity analysis and optimization of the main parameters.

3.2. Data collection and sensitivity analysis

In this section, digital twin is employed as a prediction model to evaluate process performances in a wide range of the real demo-scale

Table 5
Process streams inlet composition and operating conditions (base-case scenario).

	CH_4	CO_2	H_2S	H_2O	NaOH	T	F
Biogas	0.56	0.37	2000	0.07	–	40.0	300.00
NaOH	–	–	–	0.52	0.48	20.0	14.80
Freshwater	–	–	–	1.00	–	15.0	190.91
Clean Biogas	0.56	0.36	576	0.07		39.5	297.09
	mol/mol	mol/mol	ppm	mol/mol	w/w	°C	Nm^3/h

Table 6
Simulation and experimental data of H_2S removal efficiency.

TEST	EXPERIMENTAL DATA EFFICIENCY	DIGITAL TWIN EFFICIENCY	RELATIVE ERROR
#1	20%	19.45%	2.75%
#2	30%	31.73%	5.77%
#3	50%	52.11%	4.22%
#4	60%	61.54%	2.57%

Table 7
Nominal operating conditions of the base case scenario.

Nominal operating conditions	
Biogas temperature	40 °C
Biogas flowrate	300 Nm^3/h
H_2S inlet concentration	2000 ppm
NaOH [50% w/w] flowrate	8 L/h
Water flowrate	16 L/h

plant operating conditions. Thus, it allows to generate a large dataset without experimental campaign.

The model has been further implemented to analyse the H_2S removal efficiency after perturbating different input parameters. According to the results of the experimental campaign and literature review, the sensitivity analysis focuses on these variables.

- Biogas temperature
- Biogas flow rate
- H_2S concentration
- Sodium hydroxide flow rate
- Sodium hydroxide concentration
- Freshwater flow rate

Scrubber unit pressure sensitivity is not investigated since it is not a degree of freedom of the demo scale plant.

Each of these parameters is analysed on a wide range of values with single-directional perturbation. When an operating parameter is perturbated, the other ones keep the nominal conditions value reported in the base case scenario (Table 7). In this way, a large set of data can be collected, and it is then used to perform the sensitivity analysis. Fig. 5 illustrates the removal efficiency trends in the function of the perturbated variables. Noteworthy in Fig. 5A, the biogas temperature does not have a significant influence on efficiency. The type of bacteria that performs anaerobic digestion affects this parameter. It provides slight differences in efficiency, ranging from 85% to 72%, in the selected range of assessment (5–60 °C). Looking at the trend, the efficiency decreases by increasing the temperature: this can be explained by the inverse proportionality relations between H_2S solubility and the temperature [36]. Regarding the biogas volumetric flow rate, its variation from 50 to 1200 Nm^3/h is shown in Fig. 5B. This range is selected considering the average biogas plant capacity in Europe. From this plot, it turns out that the biogas flow rate significantly affects the column efficiency. Higher biogas flow rates result in lower absorption efficiency keeping the same working conditions. The plot reported in Fig. 5C shows how removal efficiency depends on H_2S inlet concentration. A maximum value of 12000 p.m. is chosen according to the work of Zhang et al. [32]. To maintain efficiency after H_2S concentration oscillation at the scrubbing column, factors such as sodium hydroxide or freshwater flow rates must be suitably modified. Otherwise, the 80% efficiency at 500 ppm entering, quickly drops to 40% at 12000 ppm. Fig. 5D–E highlights the removal efficiency in function of the NaOH flow rate at the different mixture concentrations. It is depictable that until reaching a threshold value of NaOH flowrate, small variations strongly affect the removal efficiency. At higher NaOH flow rates, the curve can be approximated by a slightly sloping line: even a strong sodium hydroxide variation has a small influence on the efficiency. Fig. 5F shows the dependence of the removal efficiency from the NaOH inlet concentration. Higher NaOH purity means higher scrubbing efficiency. However, commercial solutions are available with a concentration between 30 and 50%. The trend of the efficiency in the function of the freshwater is shown in Fig. 5G. An adequate removal efficiency (e.g. $>$ 70%) is achieved when the freshwater flowrate overcame the value of 100 L/h. The system requires overcoming this threshold to keep clean the solution by salts purging.

4. Conclusions

The aim of this work is the validation and optimization of a demo scale caustic scrubber unit for the removal of H_2S in a biogas stream. An experimental removal efficiency of 60% is achieved in nominal operating conditions.

The validation of technology has been addressed through the collection of field measurements in different operating conditions and the further implementation of a digital twin. Thus, it is employed as prediction model due to a strong accordance to the experimental data with a maximum relative error of 5.77%. This result proves the importance of digital twins in process engineering to forecast perturbation effects, optimize the process, and prevent safety risks. The excellent sinergies between demo-scale plant performances and digital twin has allowed to implement new analysis to validate and optimize the pilot process. Indeed, the model enables generating of a large amount of data to study the H_2S removal efficiency response to a variation of the main process parameters. All the data gathered from both the simulation and the experimental campaign have been used to perform a sensitivity analysis. The most impacting parameters identified by the sensitivity study are the sodium hydroxide flowrate and its concentration. Considering that sodium hydroxide has quite standard concentrations, the key parameter that can be manipulated to optimize the entire absorption column is the flowrate. For instance, by doubling its value from 4 to 8 L/h on the analysed plant, the efficiency drastically increased from 20% to more than 70%. The main limitation of this research is that the operating pressure of the absorption unit has not been considered as one of the investigated parameters. In fact, according to Henry's law, by increasing the pressure, the H_2S absorption is favoured. The issue is that CO_2 absorption increases at the same time, becoming more competitive. In order to prevent reduced H_2S selectivity against carbonate formation, a technological compromise must be found. Considering the complexity associated with this parameter, future studies could be dedicated to the full understanding and optimization of this operating condition.

A flexibility assessment under uncertain conditions could be performed to analyse the system behaviour.

Funding

This research did not receive any specific grant from funding agencies in the public, commercial, or not-for-profit sectors.

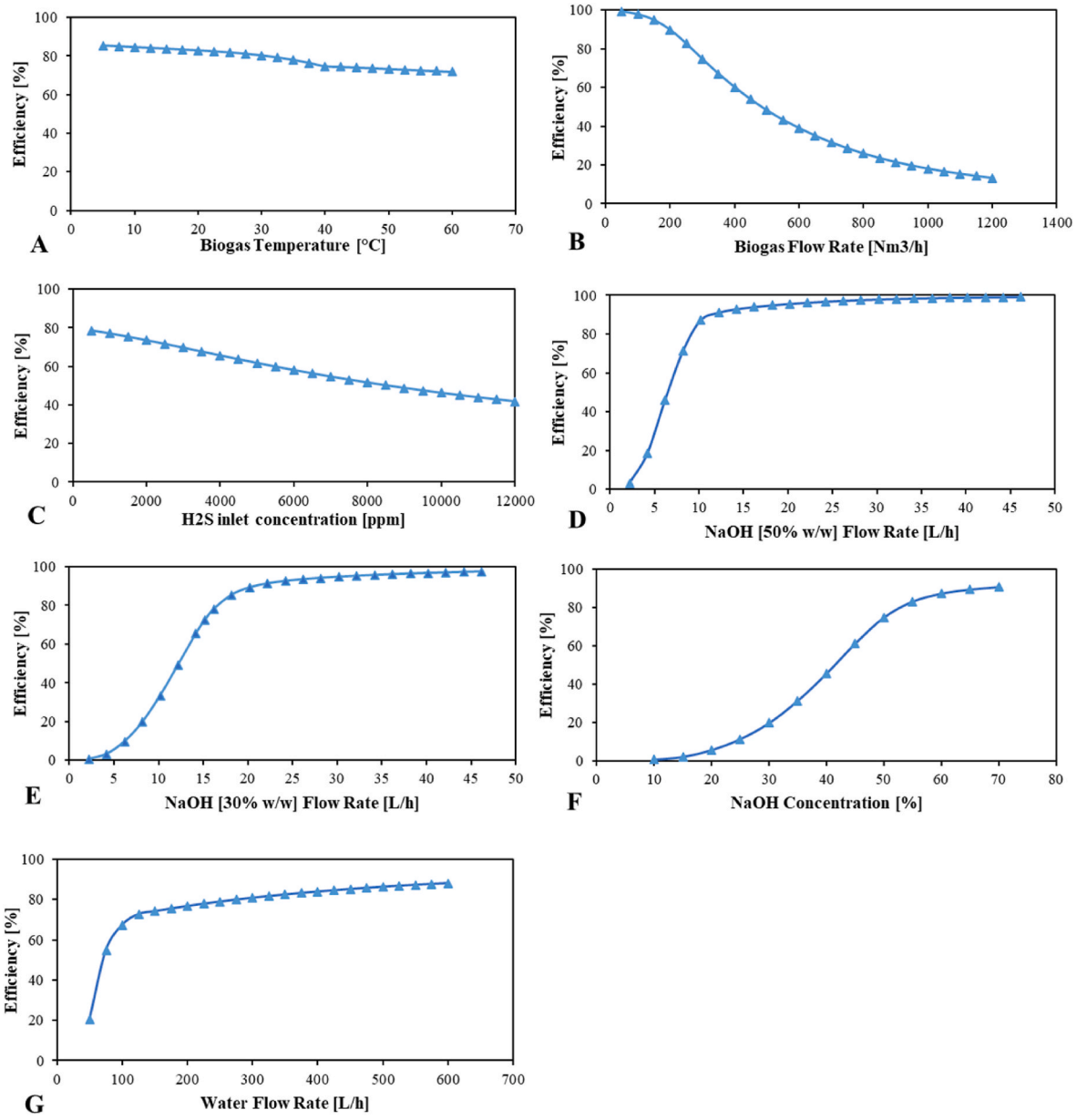

Fig. 5. Process parameters sensitivity analysis.

CRediT authorship contribution statement

Jacopo Pallavicini: Conceptualization, Investigation, Software, Methodology, Writing – original draft, Writing – review & editing. **Matteo Fedeli:** Conceptualization, Investigation, Software, Methodology, Writing – original draft, Writing – review & editing. **Giacomo Domenico Scolieri:** Conceptualization, Investigation, Software, Methodology, Writing – original draft, Writing – review & editing. **Francesca Tagliaferri:** Conceptualization, Investigation, Software, Methodology, Writing – original draft, Writing – review & editing. **Jacopo Parolin:** Conceptualization, Supervision, Project administration. **Selena Sironi:** Conceptualization, Supervision, Writing – original draft, Writing – review & editing. **Flavio Manenti:** Conceptualization, Supervision, Writing – original draft, Writing – review & editing.

Declaration of competing interest

The authors declare that they have no known competing financial interests or personal relationships that could have appeared to influence the work reported in this paper.

Appendix

Table A 1
's constant coefficients for each component

Component i	CO_2	O_2	CH_4	H_2S
Component j	H_2O	H_2O	H_2O	H_2O
Lower T [K]	273	274	275	273
Upper T [K]	500	348	353	423
a_{ij}	170.13	155.921	195.294	358.138
b_{ij}	−8477.71	−7775.06	−9111.67	−13236.8
c_{ij}	−21.9574	−18.3974	−25.0379	−55.0551
d_{ij}	0.00578075	−0,00944354	0,000143434	0.059565
e_{ij}	0	0	0	0

Table A 2
Chemical reactions involved in the absorption process

$CO_2 + 2H_2O \rightleftarrows HCO_3^- + H_3O^+$	Equilibrium	(R1)
$2H_2O \rightleftarrows OH^- + H_3O^+$	Equilibrium	(R2)
$H_2O + HCO_3^- \rightleftarrows CO_3^{2-} + H_3O^+$	Equilibrium	(R3)
$H_2O + H_2S \rightleftarrows HS^- + H_3O^+$	Equilibrium	(R4)
$H_2O + HS^- \rightleftarrows S^{2-} + H_3O^+$	Equilibrium	(R5)
$H_2S + OH^- \rightleftarrows HS^- + H_2O$	Equilibrium	(R6)
$HS^- + OH^- \rightleftarrows S^{2-} + H_2O$	Equilibrium	(R7)
$NaOH \rightarrow Na^+ + OH^-$	Dissociation	(R8)
$Na_2CO_3 \rightarrow 2Na^+ + CO_3^{2-}$	Dissociation	(R9)
$NaHCO_3 \rightarrow HCO_3^- + Na^+$	Dissociation	(R10)
$Na_2S \rightarrow S^{2-} + 2Na^+$	Dissociation	(R11)
$CO_2 + OH^- \rightarrow HCO_3^-$	Kinetic	(R12)
$HCO_3^- \rightarrow CO_2 + OH^-$	Kinetic	(R13)

Table A 3
Material and energy balances for the stream of the process simulation

Stream Name	T	P	VF	F	H2O	CO2	H3O+	OH-	HCO3-	CO3-2	NA+	O2	H2S	HS-	S-2	CH4
Units	C	Mpa		kmol/hr												
BIOGAS	40.00	0.12	0.93	26.77	1.26E-01	3.87E-01	9.55E-08	4.63E-13	9.50E-08	7.63E-14	–	3.50E-03	2.20E-03	4.83E-10	1.97E-18	4.81E-01
BOTTOM1	37.42	0.11	0.00	85.39	9.80E-01	7.00E-05	1.86E-11	1.66E-06	5.16E-03	2.43E-03	1.13E-02	7.04E-08	2.91E-06	1.27E-03	3.34E-08	1.03E-05
BOTTOM2	34.96	0.10	0.00	249.90	9.80E-01	2.38E-05	1.40E-11	1.89E-06	4.70E-03	2.89E-03	1.16E-02	6.66E-08	1.99E-06	1.09E-03	3.14E-08	9.72E-06
CLEAN	36.01	0.11	1.00	24.63	5.37E-02	4.19E-01	–	–	–	–	–	3.80E-03	1.56E-03	–	–	5.22E-01
CLEAN2	34.87	0.10	1.00	24.52	5.55E-02	4.15E-01	–	–	–	–	–	3.82E-03	1.20E-03	–	–	5.25E-01
MIX	34.66	0.10	0.00	333.23	9.80E-01	1.07E-06	9.21E-12	2.74E-06	3.64E-03	3.43E-03	1.16E-02	6.27E-08	1.25E-06	1.05E-03	4.01E-06	9.15E-06
MIX2	34.22	0.10	0.00	358.85	9.81E-01	2.21E-06	1.44E-11	1.68E-06	4.56E-03	2.56E-03	1.08E-02	6.31E-08	2.07E-06	1.06E-03	2.35E-06	9.21E-06
NAOH	15.00	0.12	0.00	2.14	7.21E-01	–	1.45E-19	1.39E-01	–	–	1.39E-01	–	–	0.00E+00	–	–
PUMPED	34.74	0.28	0.00	333.23	9.80E-01	1.07E-06	9.22E-12	2.75E-06	3.64E-03	3.43E-03	1.16E-02	6.27E-08	1.25E-06	1.05E-03	4.03E-06	9.15E-06
PURGE	34.22	0.10	0.00	27.76	9.81E-01	2.21E-06	1.44E-11	1.68E-06	4.56E-03	2.56E-03	1.08E-02	6.31E-08	2.07E-06	1.06E-03	2.35E-06	9.21E-06
RECYCLE	34.22	0.10	0.00	331.08	9.81E-01	2.21E-06	1.44E-11	1.68E-06	4.56E-03	2.56E-03	1.08E-02	6.31E-08	2.07E-06	1.06E-03	2.35E-06	9.21E-06
S1	34.74	0.28	0.00	83.31	9.80E-01	1.07E-06	9.22E-12	2.75E-06	3.64E-03	3.43E-03	1.16E-02	6.27E-08	1.25E-06	1.05E-03	4.03E-06	9.15E-06
S2	34.74	0.28	0.00	83.31	9.80E-01	1.07E-06	9.22E-12	2.75E-06	3.64E-03	3.43E-03	1.16E-02	6.27E-08	1.25E-06	1.05E-03	4.03E-06	9.15E-06
S3	34.74	0.28	0.00	83.31	9.80E-01	1.07E-06	9.22E-12	2.75E-06	3.64E-03	3.43E-03	1.16E-02	6.27E-08	1.25E-06	1.05E-03	4.03E-06	9.15E-06
S4	34.74	0.28	0.00	83.31	9.80E-01	1.07E-06	9.22E-12	2.75E-06	3.64E-03	3.43E-03	1.16E-02	6.27E-08	1.25E-06	1.05E-03	4.03E-06	9.15E-06
S5	3.00	0.10	0.95	24.52	5.55E-02	4.15E-01	8.16E-08	1.43E-14	8.14E-08	2.26E-14	–	3.82E-03	1.20E-03	1.03E-10	2.36E-20	5.25E-01
S6	5.00	0.10	0.00	1.16	9.99E-01	5.12E-04	1.68E-06	3.61E-13	1.68E-06	5.04E-13	–	1.38E-07	4.03E-06	2.22E-09	6.12E-19	2.18E-05
S7	5.00	0.10	1.00	23.37	8.77E-03	4.35E-01	–	–	–	–	–	4.01E-03	1.25E-03	0.00E+00	–	5.51E-01
S8	13.68	0.11	1.00	23.37	8.77E-03	4.35E-01	–	–	–	–	–	4.01E-03	1.25E-03	0.00E+00	–	5.51E-01
WATER	15.00	0.12	0.00	23.57	1.00E+00	–	2.78E-10	5.28E-09	–	–	5.00E-09	–	–	–	–	–

References

[1] A.I. Bayu Purwanta, M. Mellyanawaty, A. Budiman, W. Budhijanto, Techno-economic analysis of reactor types and biogas utilization schemes in thermophilic anaerobic digestion of sugarcane vinasse, Renew. Energy 201 (2022) 864–875, https://doi.org/10.1016/J.RENENE.2022.10.087.

[2] A. Furtado Amaral, D. Previtali, A. Bassani, C. Italiano, A. Palella, L. Pino, A. Vita, G. Bozzano, C. Pirola, F. Manenti, Biogas beyond CHP: the HPC (heat, power & chemicals) process, Energy 203 (2020), 117820, https://doi.org/10.1016/j.energy.2020.117820.

[3] N. Scarlat, J.F. Dallemand, F. Fahl, Biogas: developments and perspectives in europe, Renew. Energy 129 (2018) 457–472, https://doi.org/10.1016/j.renene.2018.03.006.

[4] A.S.M. Magomnang, P.E.P. Villanueva, D. Ph, Removal of Hydrogen Sulfide from Biogas Using a Fixed Bed of Regenerated Steel Wool, vols. 14–17, 2014, https://doi.org/10.17758/iaast.a1214001.

[5] A.C. Wilkie, Anaerobic digestion of dairy manure: design and process considerations, Nat. Resour. Agric. Eng. Serv. (2005) 301–312.

[6] A. Rafiee, K.R. Khalilpour, J. Prest, I. Skryabin, Biogas as an energy vector, Biomass Bioenergy 144 (2021), 105935, https://doi.org/10.1016/J.BIOMBIOE.2020.105935.

[7] CE 28/2009, CE 28/2009, 1 (2009) 32–38..

[8] P.O. Kapustenko, O.P. Arsenyeva, Process Integration for Energy Saving in Buildings and Building Complexes, Woodhead Publishing Limited, 2013, https://doi.org/10.1533/9780857097255.5.938.

[9] Sarika Jain, Global Potential of Biogas, World Biogas Assoc., 2019, pp. 1–56.

[10] I. Bragança, F. Sánchez-Soberón, G.F. Pantuzza, A. Alves, N. Ratola, Impurities in biogas: analytical strategies, occurrence, effects and removal technologies, Biomass Bioenergy 143 (2020), 105878, https://doi.org/10.1016/J.BIOMBIOE.2020.105878.

[11] H. Muche, Zimmerman, the purification of biogas, Aus Der Arbeit von GATE (1985) 34, blz.

[12] G. Tian, J. Xi, M. Yeung, G. Ren, Characteristics and mechanisms of H2S production in anaerobic digestion of food waste, Sci. Total Environ. 724 (2020), 137977, https://doi.org/10.1016/j.scitotenv.2020.137977.

[13] G. Tian, J. Xi, M. Yeung, G. Ren, Characteristics and mechanisms of H2S production in anaerobic digestion of food waste, Sci. Total Environ. 724 (2020), 137977, https://doi.org/10.1016/j.scitotenv.2020.137977.

[14] R.J. Reiffenstein, W.C. Hulbert, S.H. Roth, Toxicology of hydrogen sulfide, Annu. Rev. Pharmacol. Toxicol. 32 (1992) 109–134, https://doi.org/10.1146/annurev.pa.32.040192.000545.

[15] World Health Organization, Environmental Health Criteria 19: Hydrogen Sulfide, Environ. Heal. Criteria., 1981, https://doi.org/10.1016/0278-6915(83)90075-3.

[16] L. Chen, R. Case, L. Liu, S. Xiang, H. Castaneda, Assessment of sulfide corrosion cracking and hydrogen permeation behavior of ultrafine grain high strength steel, Corrosion Sci. 198 (2022), 110142, https://doi.org/10.1016/j.corsci.2022.110142.

[17] O.W. Awe, Y. Zhao, A. Nzihou, D.P. Minh, N. Lyczko, A review of biogas utilisation, purification and upgrading technologies, Waste Biomass Valorization 8 (2017) 267–283, https://doi.org/10.1007/s12649-016-9826-4.

[18] H.W. Ou, M.S. Chou, H.Y. Chang, Removal of hydrogen sulfide from biogas using a bubbling tank fed with aerated wastewater, Aerosol Air Qual. Res. 20 (2020) 643–653, https://doi.org/10.4209/aaqr.2019.12.0647.

[19] X. Dou, A. Veksha, W.P. Chan, W. Da Oh, Y.N. Liang, F. Teoh, D.K.B. Mohamed, A. Giannis, G. Lisak, T.T. Lim, Poisoning effects of H2S and HCl on the naphthalene steam reforming and water-gas shift activities of Ni and Fe catalysts, Fuel 241 (2019) 1008–1018, https://doi.org/10.1016/j.fuel.2018.12.119.

[20] P. Wachter, C. Gaber, J. Raic, M. Demuth, C. Hochenauer, Experimental investigation on H2S and SO2 sulphur poisoning and regeneration of a commercially available Ni-catalyst during methane tri-reforming, Int. J. Hydrogen Energy 46 (2021) 3437–3452, https://doi.org/10.1016/j.ijhydene.2020.10.214.

[21] R. Ángeles Torres, D. Marín, M. del R. Rodero, C. Pascual, A. González-Sanchez, I. de Godos Crespo, R. Lebrero, R.M. Torre, Biogas treatment for H2S, CO2, and other contaminants removal, from Biofiltration to Promis, Options Gaseous Fluxes Biotreat (2020) 153–176, https://doi.org/10.1016/b978-0-12-819064-7.00008-x.

[22] D. Fózer, M. Volanti, F. Passarini, P.S. Varbanov, J.J. Klemeš, P. Mizsey, Bioenergy with carbon emissions capture and utilisation towards GHG neutrality: power-to-Gas storage via hydrothermal gasification, Appl. Energy 280 (2020), https://doi.org/10.1016/j.apenergy.2020.115923.

[23] S. Kulawong, R. Artkla, P. Sriprapakhan, P. Maneechot, Biogas purification by adsorption of hydrogen sulphide on NaX and Ag-exchanged NaX zeolites, Biomass Bioenergy 159 (2022), 106417, https://doi.org/10.1016/J.BIOMBIOE.2022.106417.

[24] D.C. Schiavon Maia, R.R. Niklevicz, R. Arioli, L.M. Frare, P.A. Arroyo, M. L. Gimenes, N.C. Pereira, Removal of H2S and CO2 from biogas in bench scale and the pilot scale using a regenerable Fe-EDTA solution, Renew. Energy 109 (2017) 188–194, https://doi.org/10.1016/J.RENENE.2017.03.023.

[25] D.M. Cristiano, R. de A. Mohedano, W.C. Nadaleti, A.B. de Castilhos Junior, V. A. Lourenço, D.F.H. Gonçalves, P.B. Filho, H2S adsorption on nanostructured iron oxide at room temperature for biogas purification: application of renewable energy, Renew. Energy 154 (2020) 151–160, https://doi.org/10.1016/J.RENENE.2020.02.054.

[26] V. Plesu, J. Bonet, A.E. Bonet-Ruiz, A. Chavarria, P. Iancu, J. Llorens, Surrogate model for carbon dioxide equilibrium absorption using aqueous monoethanolamine, Chem. Eng. Trans. 70 (2018) 919–924, https://doi.org/10.3303/CET1870154.

[27] D. Mamrosh, K. McIntush, K. Fisher, Caustic scrubber designs for H2S removal from refinery gas streams, Am. Fuel Petrochemical Manuf. AFPM - AFPM Annu. Meet. (2014) 671–698, 2014.

[28] D. Mamrosh, T. Corporation, Consider improved scrubbing designs for acid gases, Hydrocarb. Process. 87 (2008) 69–74.

[29] J. Kang, S. Mirzaei, Z.H. Yang, Sequence-to-sequence digital twin model in chemical plants with internal rolling training algorithm, Appl. Soft Comput. 146 (2023), 110608, https://doi.org/10.1016/j.asoc.2023.110608.

[30] D. Ortiz, W.D. Chicaiza, J.M. Escaño, A.J. Gallego, A. De Andrade, J.E. Normey-rico, C. Bordons, E.F. Camacho, Digital twin of an absorption chiller for solar cooling, Renew. Energy 208 (2023) 36–51, https://doi.org/10.1016/j.renene.2023.03.048.

[31] F. Bisotti, A. Galeazzi, F. Gallo, F. Manenti, The use of digital twins to overcome low-redundancy problems in process data reconciliation, Simul. Optim. Process Eng. Benefit Math. Methods Appl. Chem. Ind. (2022) 161–199, https://doi.org/10.1016/B978-0-323-85043-8.00011-8.

[32] Y. Zhang, Y. Kawasaki, K. Oshita, M. Takaoka, D. Minami, G. Inoue, T. Tanaka, Economic assessment of biogas purification systems for removal of both H2S and siloxane from biogas, Renew. Energy 168 (2021) 119–130, https://doi.org/10.1016/J.RENENE.2020.12.058.

[33] H. Cherif, C. Coquelet, P. Stringari, D. Clodic, L. Pellegrini, S. Moioli, S. Langé, Experimental and Simulation Results for the Removal of H2S from Biogas by Means of Sodium Hydroxide in Structured Packed Columns, Icbst. 18th Inter, PARIS, France, 2016.

[34] P. Pearson Roughton, The kinetics of combination of carbon dioxide with hydroxide IONS, Angew. Chem. Int. Ed. 6 (11) (1967) 951–952, 1512–1520.

[35] R.R. Devale, Y.S. Mahajan, Materials Today : proceedings Separation of N-propyl propionate from its highly non-ideal reaction mixture : distillation using rigorous simulation, Mater. Today Proc. (2023), https://doi.org/10.1016/j.matpr.2023.07.291.

[36] J.J. Carroll, A.E. Mather, The solubility of hydrogen sulphide in water from 0 to 90°C and pressures to 1 MPa, Geochem. Cosmochim. Acta 53 (1989) 1163–1170, https://doi.org/10.1016/0016-7037(89)90053-7.